Trends in the vertical profiles of atmospheric temperature in recent decades

L.I. Nesmelova, O.B. Rodimova, and S.D. Tvorogov

Institute of Atmospheric Optics,
Siberian Branch of the Russian Academy of Sciences, Tomsk

Received September 16, 2004

The comparison of our model results obtained using a one-dimensional radiative model with the explicit temperature dependence with those calculated by global circulation models showed that the temperature trends observed in recent decades in the stratosphere and mesosphere are mostly caused by the radiative processes and result from variation of the carbon dioxide and ozone concentrations in the atmosphere. The qualitative agreement was demonstrated between the temperature trends calculated for the altitudes in the stratosphere and mesosphere and the experimental values.

Introduction

Temperature is one of the most important climatic characteristics. Its variations reflect the processes occurring in the climatic system. The adequate description of its variations in climatic models indicates the understanding of the roles of various processes in the formation of climate and allows the calculated results to be compared with the experimental ones.

The series of observation data on the vertical temperature profiles recorded by now are long enough for separation of temperature trends. In the literature, there are data on the evolution of the vertical temperature profiles for a few recent decades, obtained by processing the lidar observations, measurements with meteorological rockets and radiosondes. The analysis of such data has earlier been carried out in Refs. 1–10.

At the altitudes of the stratosphere and mesosphere, the negative temperature trend has been found. At higher altitudes, this trend generally alternates toward warming. The experimental data[1–4] on temperature variations in the stratosphere and mesosphere in the altitude range from 25 to 75 km for rather long periods (1964–1988) were obtained with meteorological rockets. For the central and upper mesosphere, the negative temperature trend was estimated as 10 K a decade. Cooling of the mesosphere (below 80 km) was also evidenced by the measurements of the height of radio wave reflection in the ionosphere's D-region in 1959–1986 [Refs. 5 and 6], and the cooling rate was determined to be 2 K a decade.

In Refs. 7 and 8, temperature variability in the middle atmosphere and its long-term tendencies were studied with a database compiled from the data of the French Rayleigh lidar at 44°N since 1979 and the sodium lidar in Colorado, USA. The tendencies of temperature variations revealed in these two datasets are roughly the same. The study was conducted in the altitude range from 35 to 80 km; the maximum cooling of 4.5 K a decade was observed at the altitudes of 60–70 km. The temperature trends in the troposphere were studied by re-analysis[10] based on the basic CARDS dataset.[9]

In the literature, there are also model calculations performed with the aid of 3D climatic models taking into account variations in the amount of absorbing substances. The results of these model calculations can be compared with the experimental temperature trends. Cooling of the stratosphere and warming of the troposphere are seen in some calculations involving the increase of the CO_2 content in the atmosphere, for example, in Refs. 11 and 12, in which a 3D global circulation model with CO_2 doubling was used. However, the values of the trends reported in different papers differ widely and, as a rule, they are insignificant to explain the observed cooling.

Warming of the mesosphere has been detected only in a few calculations. Thus, in Ref. 7 the warming is explained by aerosol emitted into the atmosphere from Mt. Pinatubo eruption. In Ref. 11 a weak warming near the northern stratopause arises upon CO_2 doubling. The decrease of the ozone concentration can also cause cooling of the stratosphere and mesosphere. In Ref. 11 the simplified global circulation model with the altitude up to 90 km and the ozone concentration decreasing by 5% a decade was used, and it was obtained that maximum cooling of 3 K a decade should be observed at the altitude of about 60 km. In Ref. 13 it was believed that the trends of the greenhouse gas concentrations are not the sole (and, likely, major) cause of the observed cooling in the mesosphere and lower thermosphere, and the effect of gravitational waves should be taken into account to explain the temperature trends.

Using the global circulation model of ICM RAS, Volodin in Ref. 14 has calculated the tendencies of temperature variation up to the altitude

0235-6880/04/11 811-05 $02.00

of 90 km with the CO_2 content increasing by 5% a decade and ozone decreasing by 5% a decade. Volcanic aerosols were ignored. The model data were zonally averaged and compared with the data of the French lidar.[7] The obtained cooling in the stratosphere and warming in the mesosphere are in a quantitative agreement with the experimental values. The temperature trends depend more strongly on O_3, rather than CO_2 variations, though they provide the same tendencies.

Global circulation models are complicated and include numerous processes. Within the framework of such models, it is difficult to estimate, to which extent the temperature variation is a consequence of dynamics, radiation, or other causes. If we want to know what physical process prevails in the formation of one or another climatic response, it is logical to use specially selected simpler models. Earlier we have formulated a simple one-dimensional radiative model of the vertical temperature profile for the qualitative study of the effect of variations of absorbing substances on the vertical temperature profile. In this paper, we used this model to study temperature trends.

Selection of the model

The model used has the form traditional of 1D radiative models for a clear sky plane-parallel atmosphere:

$$\frac{\partial(\rho c_p T)}{\partial t} = -\frac{\mathrm{d}}{\mathrm{d}H}(F_\mathrm{T} + F_\mathrm{S}), \qquad (1)$$

where T is the atmospheric temperature; F_S is the net sunlight flux; F_T is the total flux of long-wave radiation; ρ is the atmospheric density; c_p is the heat capacity at a constant pressure; H is the height. Radiative fluxes in the radiative model have a complex height dependence. To solve the above equation, the atmosphere is divided into a number of height layers, H (or p) acquires the layer number – $H_i(p_i)$, and we obtain the system of equations, whose number is equal to the number of the layers. It is a system of differential equations for layer temperatures, and, thus, the vertical temperature profile is the result of solution of a system of equations for temperatures of atmospheric layers. Radiative fluxes are traditionally expressed through the Planck's functions for individual layers and the corresponding transmission functions.

It is a specific feature of our model[15,16] that the temperature dependence of the Planck's functions is written in the explicit form and therefore the model equations become ordinary differential equations for layer temperatures. The steady state, obtained by solving the system of equations, is just the vertical temperature profile.

Main atmospheric absorbing gases (H_2O, CO_2, O_3) are considered as absorbing substances. Frequency ranges, in which the absorption of solar and thermal radiation by these gases is taken into account, are tabulated below.

Spectral ranges used in the calculations

Solar radiation

H_2O	O_3
1000–14286 cm^{-1} 10000–700 nm	14286–57143 cm^{-1} 700–175 nm

Thermal radiation

H_2O	H_2O cont	CO_2	O_3
0–3000 cm^{-1} ... – 3330 nm	540–1380 cm^{-1} 18520–7250 nm	540–800 cm^{-1} 18520–12500nm	980–1100 cm^{-1} 10200–9090 nm

Radiative fluxes are calculated by the model using the approximating equations for the transmission function of water vapor, carbon dioxide gas, and ozone, obtained by Chou with co-workers[17–19] for the short-wave and long-wave regions. Since the model ignores convection, the temperature profile near the surface is omitted. As to the stratosphere and mesosphere, despite the approximations used, namely, the neglect of the temperature dependence of the transmission functions in the course of solution, the model provides for quite a realistic behavior of the temperature with height, which can be seen from the comparison of the calculated cooling rates with the analogous data obtained by other authors. Figure 1 shows the calculated cooling rates for the atmospheric models of subarctic winter and tropical summer.

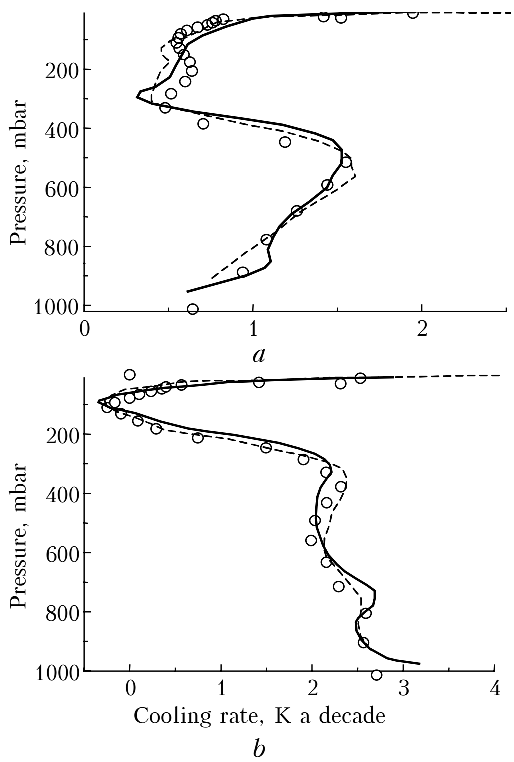

Fig. 1. IR cooling rates caused by H_2O, CO_2, and O_3 absorption and water vapor continuum absorption in the region of 0–3000 cm^{-1} as calculated for subarctic winter (*a*) and tropical summer (*b*): calculation by Galin[20] (- - - -); calculation by Chou et al.[19] (———); our calculations (○ ○ ○ ○).

Thus, the model applied rather adequately represents the known features of radiative conditions caused by the characteristics of the absorbing medium.

Calculated results

The calculations of temperature trends with our simplified 1D radiative model (without dynamics) with the same variations of CO_2 and O_3 as in Ref. 14 (5% increase of CO_2 and 5% decrease of O_3 in the standard atmosphere of mid-latitudinal summer) give the results close to the experimental data of the French lidar[7] and the data calculated by the global circulation model (GCM) of ICM RAS (Fig. 2).

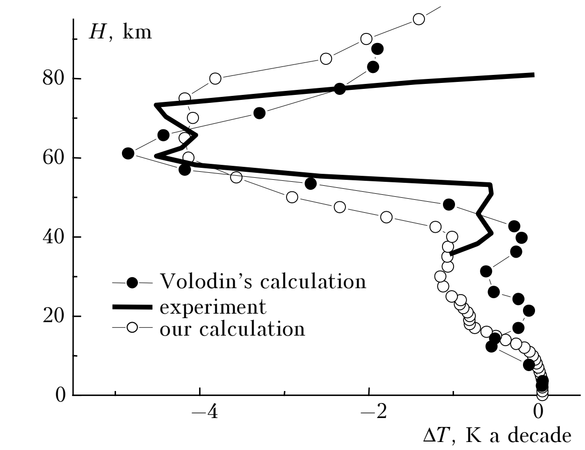

Fig. 2. Temperature trend for the altitudes of 20–80 km calculated by Volodin[14] with GCM of ICM RAS involving variations of O_3 and CO_2 content (closed circles), calculated by our model[16] (in which the trend is the difference between temperatures of steady states with standard and variable CO_2 and O_3 concentrations) with the same variations (open circles), and by the data of French lidar[7] (bold line).

It can be seen that the tendencies to the drop and increase of temperature and its relative change as a result of variation of the CO_2 and O_3 concentrations are very close to the results of the ICM 3D model. This closeness suggests that the observed temperature trends are mostly caused by radiative processes. Let us compare our results with experimental data from other papers.

Recently, specialists of the Central Aerological Observatory published their results on many-year observations of the vertical temperature profile with the aid of meteorological rockets.[4,21–23] Figure 3*b* shows the averaged data for four stations: in tropics, Arctic, Antarctic, and Volgograd. The comparison of these data with the data of lidar measurements shows that the lidar data are roughly halved as compared to the rocket measurements (Fig. 4). Unfortunately, these data cannot be directly compared with our calculations, because the presented data are averaged over seasons, while our calculations are restricted to standard model of the atmosphere. However, qualitative comparison is very interesting.

Figure 3*b* depicts the average data measured with meteorological rockets and our calculations for standard atmospheric models (Fig. 3*a*). The peak at the altitude of 60–70 km, characteristic of the lidar data and the data of rocket measurements near Volgograd, is well reconstructed in the model of mid-latitudinal summer. From the rocket measurements, it follows that this peak is observed at high altitudes both in tropics and near the poles. But, the calculations for the models of tropical summer and arctic summer and winter do not give such a significant shift of the maximum. The relative differences between the trends for different standard models may be attributed to the amount of water vapor in the model atmospheres (Fig. 5).

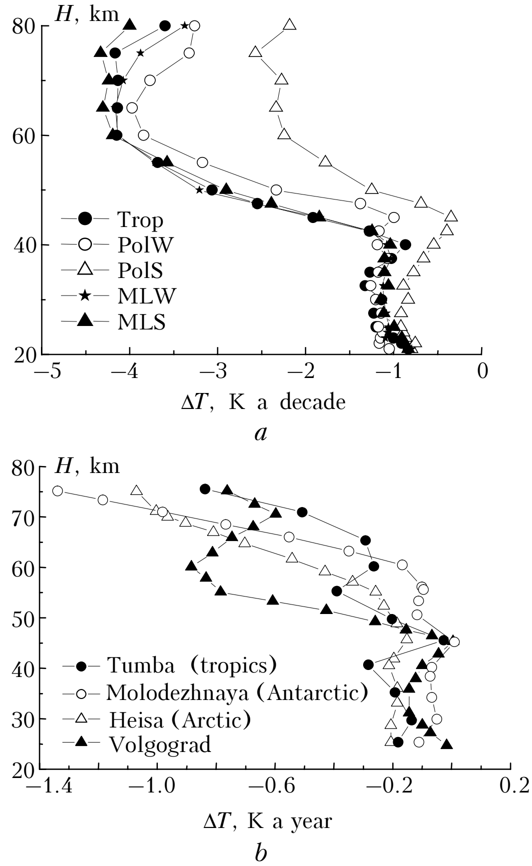

Fig. 3. Temperature trend: (*a*) calculated by our model for the standard models of the atmosphere (Trop – tropics, PolW – polar winter, PolS – polar summer, MLW – mid-latitudinal winter, MLS – mid-latitudinal summer) with variations of the O_3 and CO_2 content; (*b*) measurements with meteorological rockets.[4]

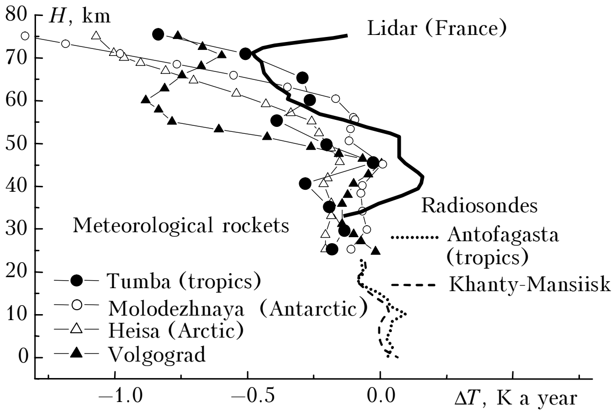

Fig. 4. Experimental trends obtained by different methods.

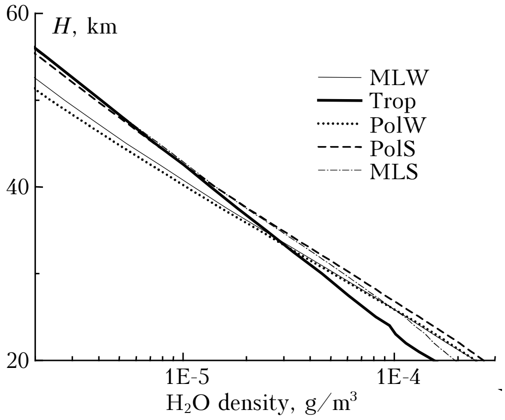

Fig. 5. Water vapor density in standard models of the atmosphere.

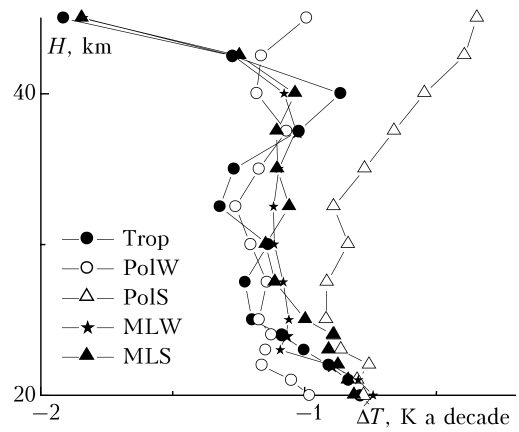

a

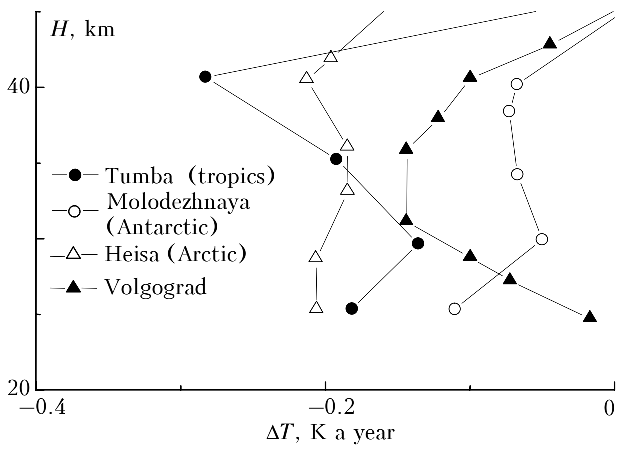

b

Fig. 6. Temperature trends for the altitudes of 20–45 km (see Fig. 3).

Indeed, at the altitudes of 50–80 km, the trend curves re-inverse to the water vapor density curves, where the latter are quite regular. In the region of 30 km and lower, the water vapor density curves get entangled, and the behavior of the trends is very irregular as well, though some qualitative similarities can be seen (Fig. 6).

Although it was already mentioned above that our model does not suit the consideration of the troposphere, it is interesting to compare the calculated results with the experimental temperature trends obtained from aerological data. Figure 7 demonstrates the results of such a comparison.

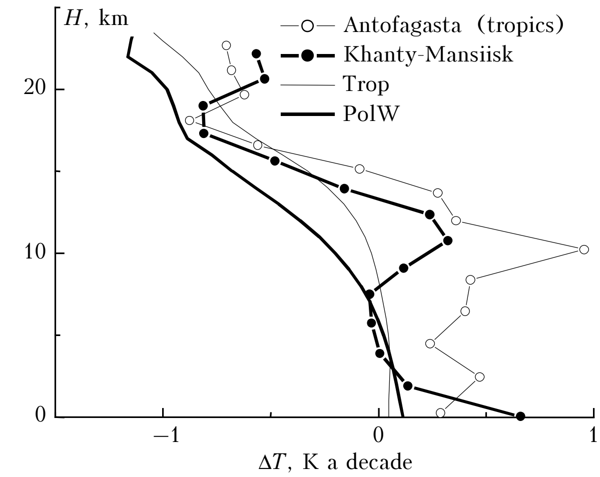

Fig. 7. Temperature trends calculated by our model for the standard atmospheric models and those obtained from the radiosonde data.[10]

Conclusions

It should be noted that simple models, similar to our model, certainly could not ensure very accurate qualitative agreement. This model serves for quick calculation of the vertical temperature profile for a large number of studied situations and, thus, for detection of qualitative features of the temperature behavior in a wide range of variability of atmospheric parameters, such as the concentrations of minor gaseous constituents. The agreement between our calculations and the values obtained in 3D global circulation models indicates that the temperature trends in the stratosphere and lower mesosphere are mostly of radiative nature and can be a result of variation of the ozone and carbon dioxide content in the atmosphere.

The comparison of the temperature trends calculated based on our model with the experimental data obtained by different methods demonstrates qualitative agreement between them at the altitudes of the stratosphere and mesosphere. This comparison is difficult, because in our calculations we have to use the temperature, pressure, and concentration distributions for standard atmospheric models corresponding to fixed seasons and latitudes. At the same time, the experimental data available in the literature not always correspond to these conditions. We hope that further investigations of temperature trends with the aid of our model will reveal the regularities, which can be attributed to radiative processes and which cannot be explained by these processes.

References

1. J.K. Angell, Mon. Weather. Rev. **115**, 2569–2577 (1987).
2. G.A. Kokin, E.V. Lysenko, and S.Kh. Rozenfeld, Izv. Akad. Nauk SSSR, Fiz. Atmos. Okeana **26**, No. 7, 702–710 (1990).
3. G.A. Kokin and E.V. Lysenko, J. Atmos. Terr. Phys. **56**, 1035–1040 (1994).
4. E.V. Lysenko, G.G. Nelidova, and A.M. Prostova, Izv. Ros. Akad. Nauk, Fiz. Atmos. Okeana **33**, No. 2, 241–249 (1997).
5. G. Cossart and J. Taubenheim, J. Atmos. Terr. Phys. **49**, 303–307 (1987).
6. J. Taubenheim, G. von Cossart, and G. Entzian, Adv. Space Res. **10**, No. 10, 171–174 (1990).
7. P. Keckhut, A. Hauchecorne, and M.L. Chanin, J. Geophys. Res. D **100**, No. 9, 18887–18897 (1995).
8. C.Y. She, J.R. Yu, D.A. Krueger, R. Roble, P. Keckhut, A. Hauchecorne, and M.L. Chanin, Geophys. Res. Lett. **22**, 377–390 (1995).
9. O.A. Alduchjv and R.E. Eskrige, "*Complex quality control of upper air parameters on mandatory and significant levels for the CARDS dataset*," NCDC Report NTISPB 97132286 (1996), 125 pp.
10. V.M. Khan, A.M. Sterin, and K.G. Rubinshtein, Meteorol. Gidrol., No. 12, 5–18 (2003).
11. D. Rind, R. Suozzo, N.K. Balacahadran, and M.J. Pratcher, J. Atmos. Sci. **47**, 475–491 (1990).
12. J. Bremer and U. Berger, in: *Proc. First Int. Workshop on Long-Term Changes and Trends* (Pune, 1999).
13. A.N. Gruzdev and G.P. Brasseur, in: *Abstracts of X Joint International Symposium on Atmospheric and Ocean Optics. Atmospheric Physics* (Tomsk, 2003), pp. 150–151.
14. E.M. Volodin, Izv. Ros. Akad. Nauk, Fiz. Atmos. Okeana **36**, No. 5, 617–625 (2000).
15. O.B. Rodimova, Atmos. Oceanic Opt. **14**, Nos. 6–7, 439–443 (2001).
16. L.I. Nesmelova, O.B. Rodimova, and S.D. Tvorogov, Vychisl. Tekhnol., Spec. Issue **7**, 71–77 (2002).
17. M.-D. Chou and K.T. Lee, J. Atmos. Sci. **53**, No. 8, 1203–1208 (1996).
18. M.-D. Chou, J. Atmos. Sci. **49**, 762–772 (1992).
19. M.-D. Chou, W.L. Ridgway, and M.M.-H. Yan, J. Atmos. Sci. **50**, No. 14, 2294–2303 (1993).
20. V.Ya. Galin, Izv. Ros. Akad. Nauk, Fiz. Atmos. Okeana **34**, No. 3, 380–389 (1998).
21. E.V. Lysenko, G.G. Nelidova, and A.M. Prostova, Izv. Ros. Akad. Nauk, Fiz. Atmos. Okeana **33**, No. 2, 250–257 (1997).
22. E.V. Lysenko and V.Ya. Rusina, Izv. Ros. Akad. Nauk, Fiz. Atmos. Okeana **38**, No. 3, 337–346 (2002).
23. E.V. Lysenko and V.Ya. Rusina, Izv. Ros. Akad. Nauk, Fiz. Atmos. Okeana **38**, No. 3, 347–353 (2002).